Electronic Supplementary Information

Ultrahigh power factor and flexible silver selenide-based composite film for thermoelectric devices

Yao Lu[1], Yang Qiu[2], Kefeng Cai[1*], Yufei Ding[1], Mengdi Wang[3], Cong Jiang[1], Qin Yao[3], Changjun Huang[1], Lidong Chen[3*], Jiaqing He[2*]

[1] Key Laboratory of Advanced Civil Engineering Materials, Ministry of Education, School of Materials Science & Engineering, Tongji University, 4800 Caoan Road, Shanghai 201804, China

[2] Materials Characterization and Preparation Center and Department of Physics, Southern University of Science and Technology, Shenzhen 518055, China

[3] State Key Laboratory of High Performance Ceramics and Superfine Microstructure, Shanghai Institute of Ceramics, Chinese Academy of Science, Shanghai, 200050, China

Corresponding authors

*Email address: kfcai@tongji.edu.cn; hejq@sustc.edu.cn; cld@mail.sic.ac.cn

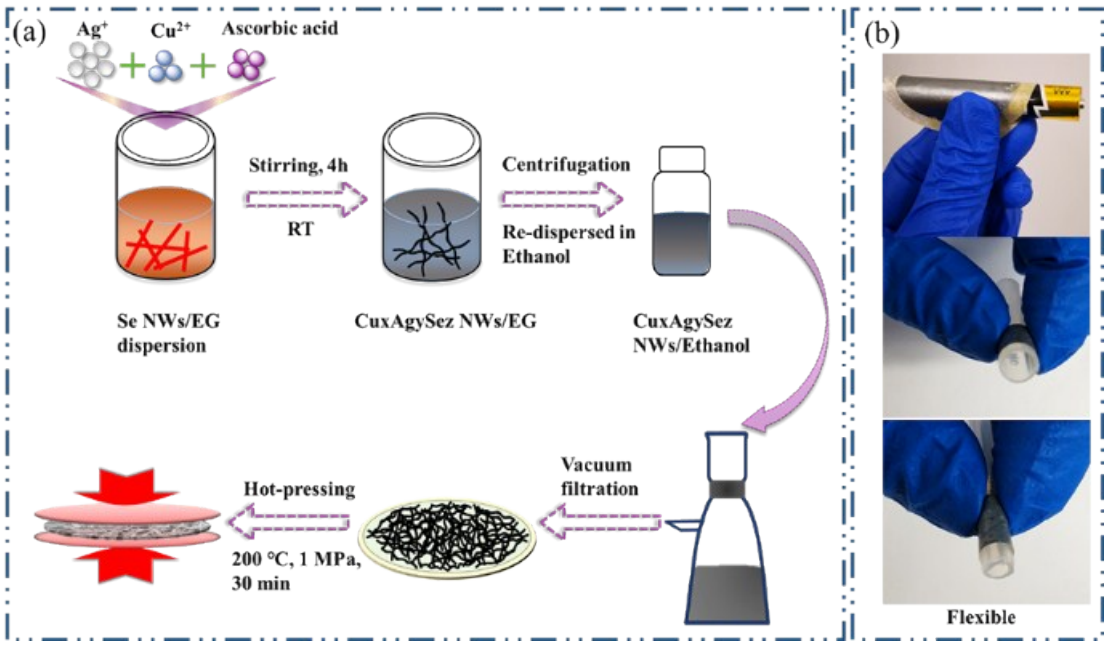

Fig. S1 (a) Fabrication of the CuxAgySez film supported by porous nylon membrane, (b) photographs showing the flexibility of the CuxAgySez film.

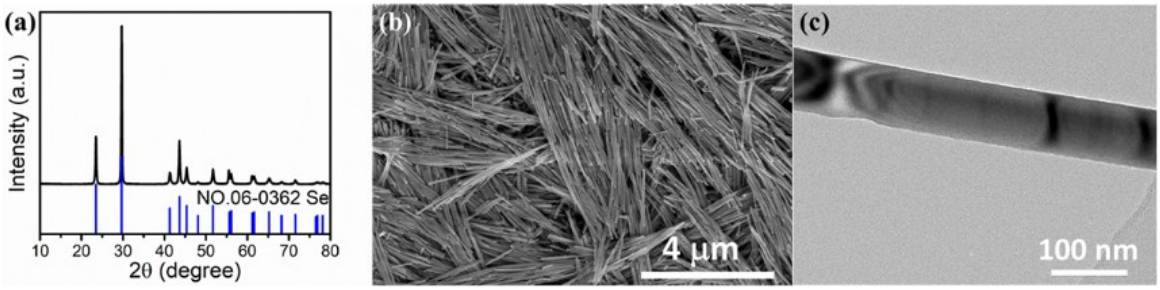

Fig. S2 (a) XRD pattern, (b) FESEM image and (c) TEM of the as-prepared Se NWs.

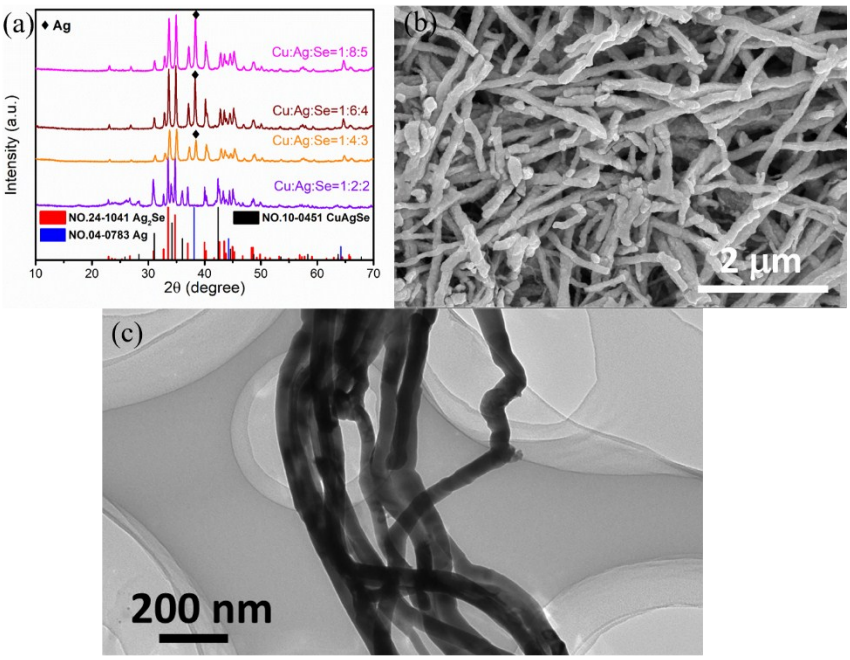

Fig. S3 (a) XRD patterns of the CuxAgySez NWs, (b) typical surface FESEM image of the CuxAgySez NWs, (c) a TEM image of the CuxAgySez NWs.

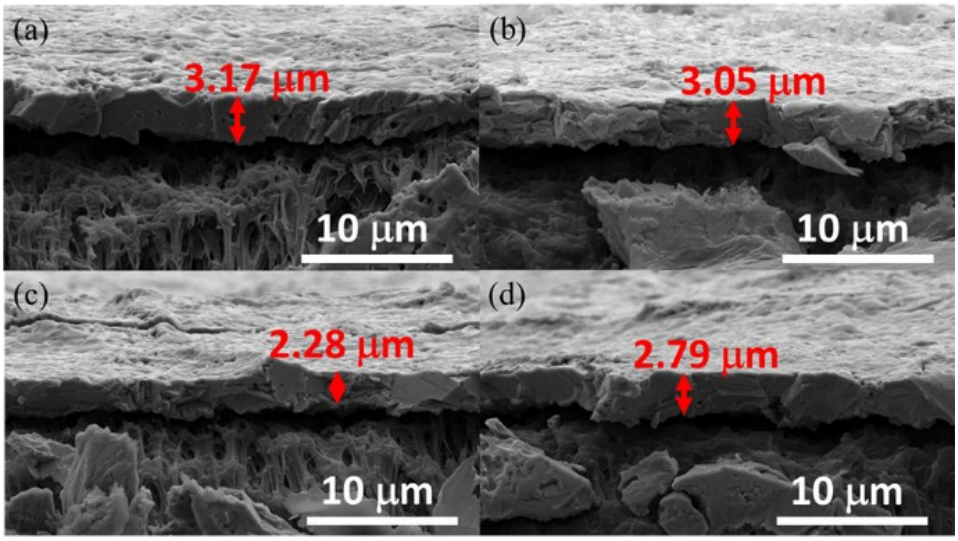

Fig. S4 Fractured surface SEM images of the Cu1Ag2Se2 (a), Cu1Ag4Se3 (b), Cu1Ag6Se4 (c) and Cu1Ag8Se5 (d) composite films.

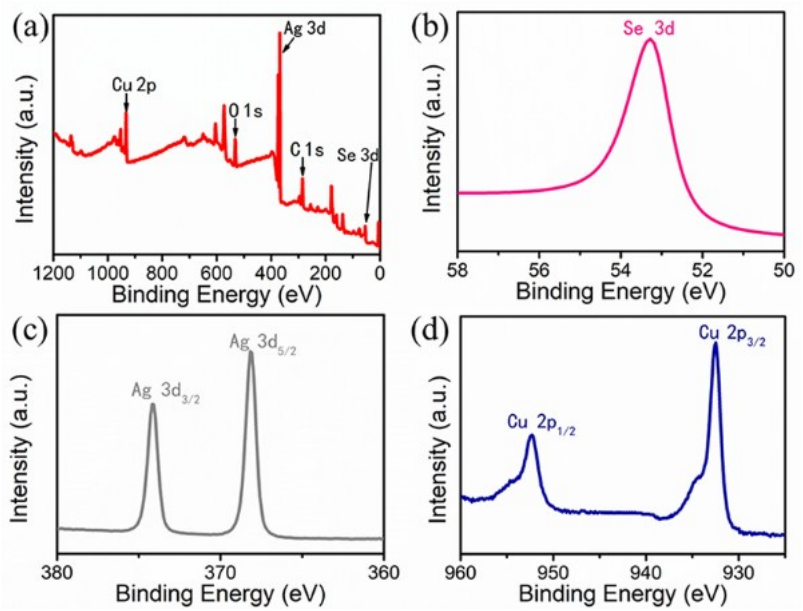

Fig. S5 XPS spectra of the Cu1Ag4Se3 sample (a) XPS survey spectra, (b) Se 3d spectra, (c) Cu 2p spectra, (d) Cu 2p spectra.

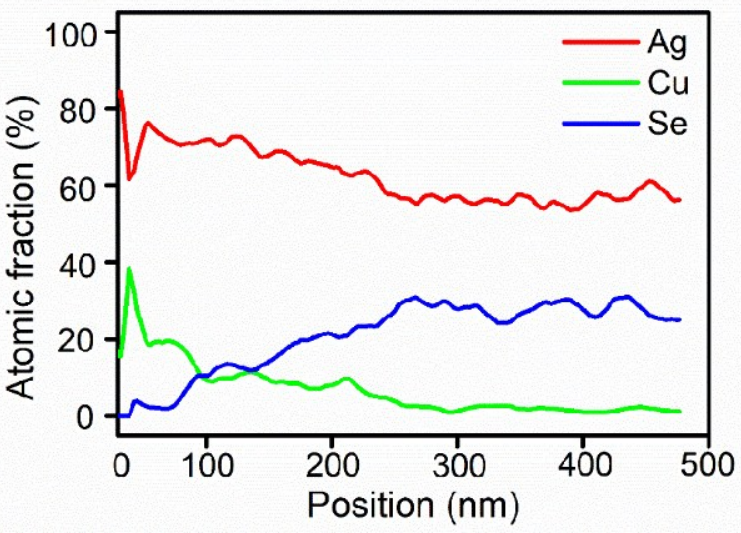

Fig. S6 STEM-EDS line scan profile along the black arrow in Fig. 4(b).

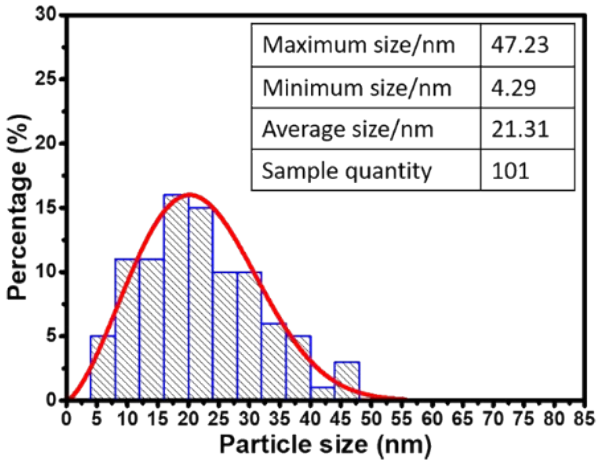

Fig. S7 The size and distribution of the Ag nanoparticles.

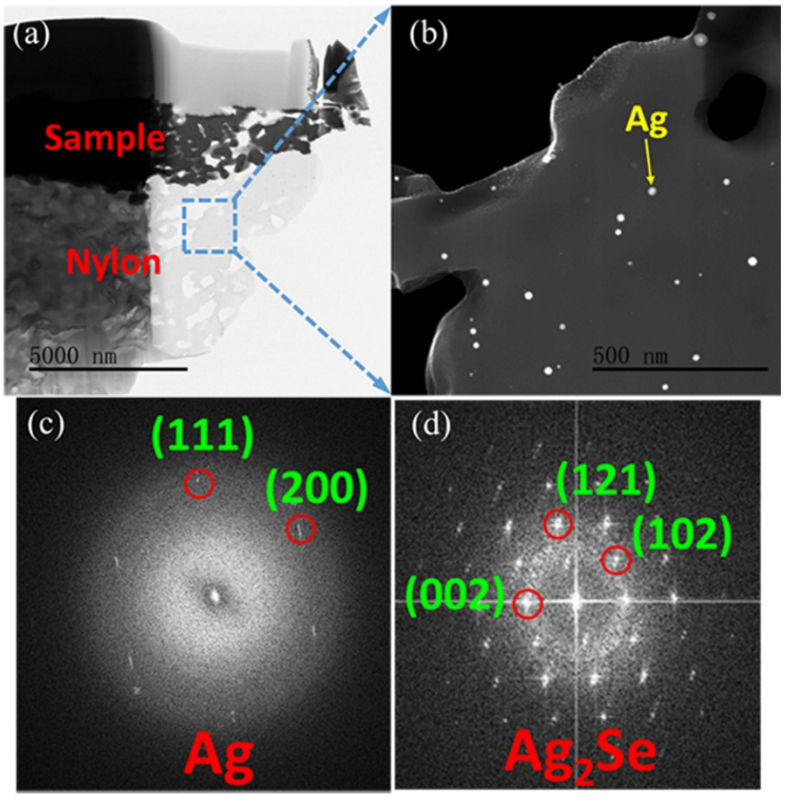

Fig. S8 (a) A bright-field STEM image of the Cu1Ag4Se3 sample prepared by FIB, (b) an overview HAADF-STEM image, (c) a FFT image of Ag in Fig. 4(c), (d) a FFT image of Ag_2Se in Fig. 4(e).

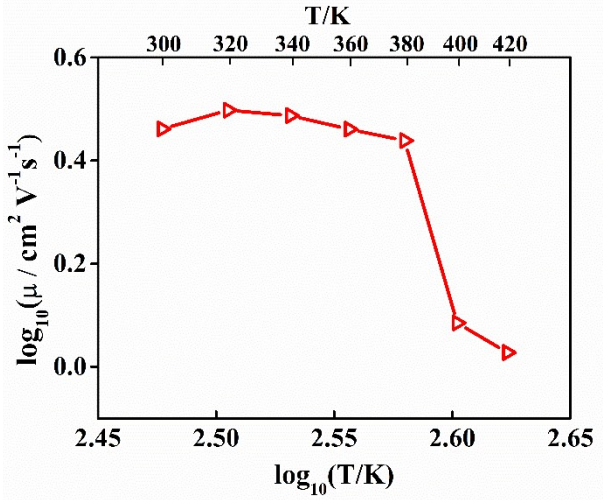

Fig. S9 The slopes of log-log plots of Hall mobility versus temperature indicate the dominant scattering mechanism.

Fig. S10 The electrical resistance of the Cu1Ag4Se3 hybrid film in the original flat state, bending deformation state and the recovery flat state. The two ends of the film were jointed with two conductor wires using the Ag adhesive.

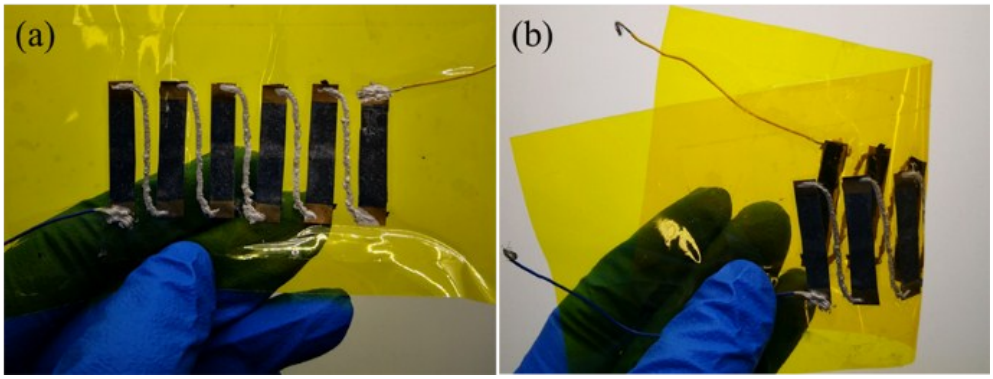

Fig. S11 Photograph of the fabricated TE device with flat state (a) and the folded state (b).

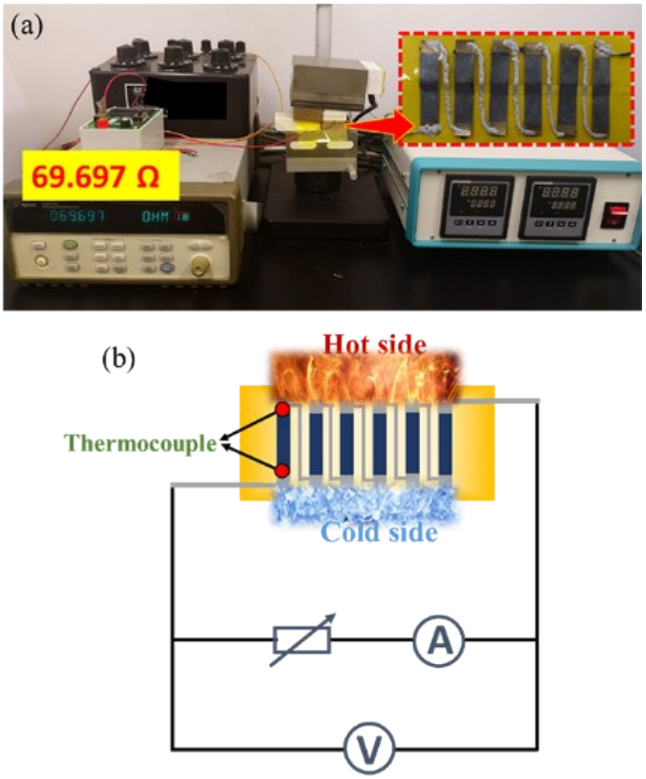

Fig. S12 Home-made apparatus for the performance measurement of TE generator. (a) The digital photo showing the internal resistance of the as-prepared TE device, (b) electrical circuit schematic diagram.

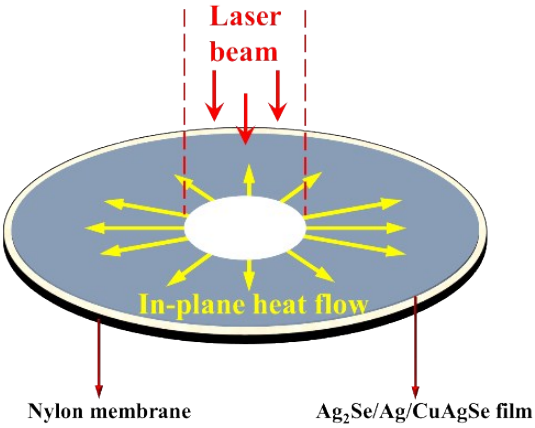

Fig. S13 Schematic diagram of the in-plane heat flow.

Table S1 The integral area of the Ag peak and the strongest peak of Ag_2Se calculated from Fig. 1(a).

Film	I_{Ag}	I	I_{Ag}/I (%)
Cu1Ag4Se3	35638	75068	38.2%
Cu1Ag6Se4	22924	42570	42.7%
Cu1Ag8Se5	17178	34683	26.1%

Table S2 The parameters of in-plane thermal conductivity of the Ag_2Se-based composite film with nylon and the nylon at room temperature.

Film	d ($g\ cm^{-3}$)	Cp ($J\ g^{-1}\ K^{-1}$)	D ($mm^2\ s^{-1}$)	κ ($W\ m^{-1}\ K^{-1}$)
Nylon	0.65	0.8536	0.533	0.2957
Ag_2Se/CuAgSe/Ag/Nylon	1.28	1.319	0.783	1.32

Table S3 The temperatures of the hot and the cold side of the TE device.

T_h (°C)	T_c (°C)	ΔT(°C)
44	25.7	18.3
54.3	26.2	28.1
66.2	27.1	39.1
73.6	28.5	45.1